

# Anaplastic thyroid carcinoma and foscarnet use in a multitarget treatment documented by <sup>18</sup>F-FDG PET/CT

## A case report

Elisa Giannetta, MD, PhD<sup>a</sup>, Andrea M. Isidori, MD, PhD<sup>a</sup>, Cosimo Durante, MD, PhD<sup>b</sup>, Cira Di Gioia, MD, PhD<sup>c</sup>, Flavia Longo, MD, PhD<sup>c</sup>, Vincenzo Tombolini, MD, PhD<sup>c</sup>, Nadia Bulzonetti, MD, PhD<sup>c</sup>, Chiara Graziadio, MD<sup>a</sup>, Riccardo Pofi, MD<sup>a</sup>, Daniele Gianfrilli, MD, PhD<sup>a</sup>, Antonella Verrienti, PhD<sup>d</sup>, Raffaella Carletti, biomedical laboratory technician<sup>c</sup>, Sebastiano Filetti, MD, PhD<sup>b</sup>, Andrea Lenzi, MD, PhD<sup>a</sup>, Alberto Baroli, MD, PhD<sup>d,\*</sup>

### Abstract

**Rationale:** The case reported the rapid remission of disease recurrence achieved adding foscarnet, a DNA polymerase inhibitor that interacts with fibroblast growth factor 2, to low molecular weight heparin and sunitinib for the first time in a patient with an anaplastic thyroid cancer (ATC).

**Patient concerns:** A 65-year-old woman with a multinodular goiter referred for a rapid enlargement of a nodule. Histological examination revealed an ATC with a little area of papillary thyroid cancer (PTC). The patient was resistant to selective single-target treatment.

**Diagnoses:** Immunophenotyping and gene analyses found a significant increase in FGF2 and FGFR1 expression in the primary ATC area (FGF2 = 38.2 ± 6.2% in ATC vs 34.6 ± 6.0% in the differentiated area of PTC,  $P < 0.05$ ; FGFR1: 41.7 ± 6.0% in ATC vs 34.4 ± 4.2% in PTC,  $P < 0.001$ ) and in metastatic neck lymph nodes ( $P < 0.001$  vs normal control tissues). Unlike conventional imaging, <sup>18</sup>F-FDG PET/CT with PERCIST 1.0 criteria promptly and quantitatively detected disease recurrence and remission before and after multitarget therapy, combining anatomic, metabolic, and functional data.

**Interventions:** Foscarnet was administered given the positivity for FGF2, FGFR1 and FGFR4 in ATC. Low molecular weight heparin and Sunitinib were coadministered to limit metastatic progression and on neck tumor mass, respectively.

**Outcomes:** The rationale for the clinical response to this innovative multitarget association with foscarnet is based on the histological and genetic finding that fibroblast growth factors and their receptor super-family are up-regulated in the primary anaplastic thyroid tumor and in the metastatic lymph node of our patient.

**Lessons:** We propose that fibroblast growth factors and their receptor super-family play a key role as potential therapeutic targets in anaplastic thyroid cancer and the positive relevance of this suggestion for patient care, especially for an individualized management.

**Abbreviations:** ATC = anaplastic thyroid cancer, BTA = British Thyroid Association, CT = computed tomography, DCI = histone deacetylase inhibitor, FGF = fibroblast growth factor, FGFR = fibroblast growth factors receptor, HBD = heparin-binding domain, LMWH = low molecular weight heparin, PERCIST = Positron Emission Tomography Response Criteria in Solid Tumors, PTC = papillary thyroid carcinoma, SUV = standardized uptake value.

**Keywords:** anaplastic thyroid cancer, FGFRs, heparin, PERCIST, sunitinib

Editor: László Géza Boros.

Drs EG and AMI contributed equally to this work.

The authors have no conflicts of interest to disclose.

Supplemental Digital Content is available for this article.

<sup>a</sup> Department of Experimental Medicine, <sup>b</sup> Department of Internal Medicine and Clinical Specialties, <sup>c</sup> Department of Radiology, Anatomopathology and Oncology, Sapienza University of Rome, Rome, <sup>d</sup> Nuclear Medicine Unit, Department of Interventional Oncology, Azienda Ospedaliera Ospedale di Circolo di Busto Arsizio Varese, Busto Arsizio, Varese, Italy.

\* Correspondence: Alberto Baroli, Oncologic PET CT Center, Nuclear Medicine Unit, Department of Oncology, ASST-VALLEOLONA, via Amaldo da Brescia n 1, 21052 Busto Arsizio, Varese, Italy (e-mail: alberto.baroli@asst-valleolona.it).

Copyright © 2017 the Author(s). Published by Wolters Kluwer Health, Inc.

This is an open access article distributed under the terms of the Creative Commons Attribution-Non Commercial-No Derivatives License 4.0 (CCBY-NC-ND), where it is permissible to download and share the work provided it is properly cited. The work cannot be changed in any way or used commercially without permission from the journal.

Medicine (2017) 96:6(e5621)

Received: 9 May 2016 / Received in final form: 13 October 2016 / Accepted: 15 November 2016

<http://dx.doi.org/10.1097/MD.0000000000005621>

## 1. Introduction

Anaplastic thyroid cancer (ATC) is a rare uncontrolled aggressive disease characterized by local invasion of upper airways and dissemination of distant metastases. Its high speed of progression and uncontrolled growth at the neck level soon cause the patient's death by suffocation. The paucity of cases, the high lethality (median survival <6 months), and the histrionic behavior of the disease that select resistant clones during its growth and proliferation explain the lack of effective treatments.<sup>[1,2]</sup> The conventional therapeutic considers ATC as systemic disease at the time of diagnosis and includes cytoreductive surgical resection and chemoradiation. Several studies have shown increased expression of the multidrug-resistant-associated protein in ATC cell lines that could explain the poor outcomes with traditional therapies. The FACT Trial<sup>[3,4]</sup> and a phase II study<sup>[5]</sup> demonstrated the efficacy and safety of fosbretabulin (Combreastatin A-4 phosphate, CA4P, Zybrestat) in patients with advanced ATC and whether fosbretabulin, indicating the prognostic value of serum soluble intracellular adhesion molecule-1 (sICAM) as a therapeutic biomarker. These data need for further prospective validation.

Recent molecular studies on ATC revealed a dysregulation of fibroblast growth factors (FGF) and their receptor super-family (FGFR).<sup>[6]</sup> FGF2 and FGFR1 are overexpressed in ATC and are involved in cell proliferation. FGFR4 is strongly expressed in the more aggressive primary thyroid tumors and is functionally related to ATC aggressiveness.<sup>[6]</sup> FGF2 activates ERK1/2, a major controller of cell proliferation,<sup>[7]</sup> through 4 high-affinity tyrosine kinase receptors (FGFR1-4). Loss of FGF-FGFR system regulation may involve an autocrine/paracrine loop producing neoplastic transformation and tumor dedifferentiation.<sup>[6]</sup> A recent multicenter randomized clinical trial proposed that the success of lenvatinib in improving progression-free survival and response rate in radioiodine-refractory thyroid cancer is due to the inhibition of specific targets, including FGFRs.<sup>[8]</sup>

FGF/FGFR manipulation is a potential new additional therapeutic target. Only 2 studies have explored this possibility *in vitro* in cell lines derived from ATC. The first<sup>[1]</sup> achieved significant proliferation arrest with high doses of FGFR4 tyrosine kinase inhibitor (PD173074); the second<sup>[7]</sup> showed a reduction in FGF2-induced proliferation upon treatment with foscarnet.

Foscarnet is a broad-spectrum antiviral.<sup>[9]</sup> It competes with ATP on the same FGF2 heparin-binding domain (HBD), reducing the bioactivity of the growth factor.<sup>[7]</sup> However, foscarnet alone cannot arrest cell growth, suggesting that multiple targets are needed.<sup>[7]</sup>

We report the first administration of foscarnet in a combinatorial treatment regimen targeting different ATC pathogenic mechanisms, using PERCIST 1.0 (positron emission tomography response criteria in solid tumors) criteria in monitoring local and systemic response to therapies.

## 2. Case report

Written informed consent was obtained from both the patient and the family for publication of this manuscript and accompanying images. A 65-year-old Caucasian woman with a 10-year history of multinodular goiter presented for the rapid enlargement of a nodule. Patient did not take any medications, and in her family history only the father died of lung sarcoma. Fine-needle aspiration cytology of a massive hypoechoic nodule showed a papillary thyroid carcinoma (PTC) (Thy 5, British Thyroid Association, BTA-RCP 2007) with "tall cells" and nuclear giant

cells. Suspicious lymph node cytology was inconclusive (Tg wash testing <0.1 ng/mL). Whole body X-ray computed tomography (CT) and brain magnetic resonance imaging were negative.

The patient underwent total thyroidectomy and lymphadenectomy (central and right laterocervical compartments). Histological examination revealed an ATC (58 mm) with an area of papillary thyroid cancer PTC (18 mm) (Fig. 1A–B, E–F), and invasion of surrounding soft tissue and muscle; 13 of 20 metastatic cervical lymph nodes showed an extensive cystic necrotic core area bordered by neoplastic cells of epithelial appearance (pT4b pN1b according to 2009 AJCC/UICC TNM staging system, seventh edition). Immunostained ATC was positive only for AE1/AE3 cytokeratins and for TP53, with high Ki67 (MIB-1) index (Fig. 1C and D). PTC was positive for AE1/AE3 cytokeratins, cytokeratin-19, TTF-1, galectin-3 and HMBE-1, B-RAF and negative for thyroglobulin and TP53, with low Ki67 index (Fig. 1E–H). For major details, see the Methods section in the Supplements, <http://links.lww.com/MD/B531>.

An <sup>18</sup>F-FDG PET/CT scan 3 weeks postsurgery showed regrowth of "new pathological tissue" on the right neck. PET/CT (<sup>18</sup>F-FDG, 4 MBq/kg) was performed using Biograph PET/CT system (Siemens, ASST Valleolona). Low-dose CT acquisition was performed first, without any breath-holding instructions. A PET emission scan was performed immediately after the CT, without changing the patient's position. CT data were used for attenuation correction.

Intensity-modulated radiation therapy (6 MV X-ray beam, 60 Gy in fractionated doses, 300 cGy daily) with radiosensitizing low-dose chemotherapy (Cisplatin 50 mg/m<sup>2</sup>/wk-4 cycles) in association with the histone deacetylase inhibitor (DCI) valproic acid<sup>[10]</sup> continuous daily administration was promptly commenced. At the 3-week follow-up, <sup>18</sup>F-FDG PET/CT demonstrated complete remission in the neck, and systemic disease progression with lung metastases (pT4b pN1b M1).

First-line systemic chemotherapy with paclitaxel (80 mg/mq) was not well tolerated. Radiosurgery with CyberKnife was performed for the largest metastases in the right lung (5400 and 4500 cGy respectively in fractionated doses subsequently administered- Cyberknife VSI 9.6 system).

Two-weeks postradiosurgery, <sup>18</sup>F-FDG PET/CT revealed an improvement in the pulmonary lesions but systemic disease progression in the lung and right kidney (40 mm).

Given the intolerance to conventional chemotherapy and the systemic disease progression, baseline ICAM-1 level was measured in order to favor a prompt shift to new potential more effective therapy (see Methods section in the Supplements, <http://links.lww.com/MD/B531>). Given the intermediate value of serum ICAM levels of 293 ng/mL (226.18 < ICAM ≤ 303.62 ng/mL),<sup>[5]</sup> Zybrestat (fosbretabulin, combrestatin A4 phosphate-CA4P) (60 mg/m<sup>2</sup> weekly) was started (intravenously over 10 minutes on days 1–8–15 of 21-day cycle),<sup>[3,4]</sup> associated with Taxotere and Cisplatin every 3 weeks (OXiGENE Inc supplied Zybrestat for compassionate use). After 4 weeks, <sup>18</sup>F-FDG PET/CT revealed recurrence in the neck, rapidly progressing pulmonary and kidney metastases and bone involvement in the right scapula and left femur (Fig. 2A–C).

Parallel, gene sequencing and gene expression analyses were performed to identify the targets involved. BRAF exon 15 was amplified and sequenced on DNA extracted from PTC and ATC formalin-fixed, paraffin embedded tumor tissues. In the differentiated PTC area, somatic mutation was detected in exon 15 at codon 600 (GTG> GAG; Val> Glu heterozygous) of the B-RAF gene, but was not found in the ATC area (Fig. 3A).<sup>[11]</sup>

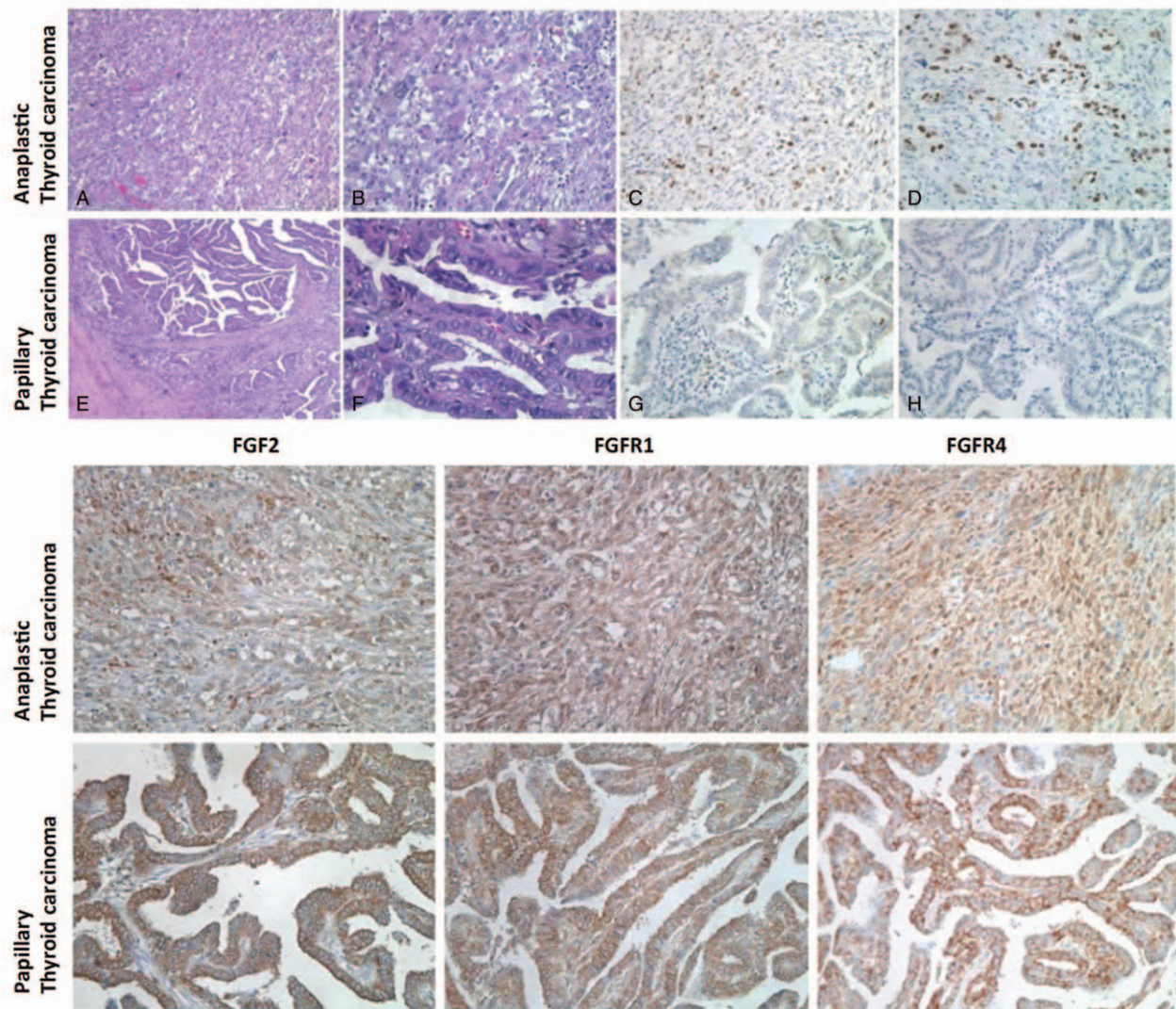


**Figure 1.** Histologic analyses with immunophenotyping. Top: anaplastic thyroid carcinoma with a differentiated component of papillary thyroid carcinoma. ATC was composed of a mixture of spindle cells often with sarcomatoid appearance and epithelioid cells, frequently with squamoid features (H&E, A  $\times 10$ , B  $\times 40$ ); in some areas the neoplastic cells were also arranged in an angiosarcoma-like pattern. There were areas of coagulative necrosis, hemorrhage, and frequent mitotic activity. The neoplastic cells showed high Ki67 (MIB-1) index (C  $\times 20$ ) and positivity for TP53 (D  $\times 20$ ). PTC was the well-differentiated, classic variant (H&E, E  $\times 10$ , F  $\times 40$ ), and showed very low Ki67 index (G  $\times 20$ ) and negativity for TP53 (H  $\times 20$ ). Bottom: immunohistochemical evaluation of FGF2, FGFR1, and FGFR4 in anaplastic thyroid carcinoma and in well-differentiated associated component. We observed stronger staining for all 3 antibodies in ATC ( $\times 20$ ). ATC = anaplastic thyroid cancer, FGFR = fibroblast growth factors receptor, PTC = papillary thyroid carcinoma.

Gene expression analysis for FGF2 and FGFR1 genes was studied. Total RNA was extracted from the ATC fresh-frozen lymph node tissue and reverse transcription was performed as previously described.<sup>[12,13]</sup> cDNA from lymph node metastasis was analyzed using Taqman Gene Expression Assays-on-Demand (Life Technologies). Both FGF2 and FGFR1 mRNAs were found in metastatic neck lymph nodes, with significant higher levels of FGFR1 ( $P < 0.001$ ) in comparison to normal control tissues (Fig. 3B). For major details, see Methods section in the Supplements, <http://links.lww.com/MD/B531>.

Tumor sections were deparaffinized and stained with antibodies. Immunostaining for anti-FGF2, anti-FGFR1, and anti-FGFR4 antibodies was quantified and expressed as the ratio of stained area to total area (%). Statistical analysis was performed using *t* test. *P* values  $< 0.05$  were regarded as statistically significant. There was a significant increase in FGF2, FGFR1, and FGFR4 expression in the ATC versus the PTC: FGF2:  $38.2 \pm$

$6.2\%$  in ATC versus  $34.6 \pm 6.0\%$  in PTC,  $P < 0.05$ ; FGFR1:  $41.7 \pm 6.0\%$  in ATC versus  $34.4 \pm 4.2\%$  in PTC,  $P < 0.001$ ; FGFR4:  $38.2 \pm 3.3\%$  in ATC versus  $32.7 \pm 7.6\%$  in PTC,  $P < 0.005$  (Figs. 1-51, <http://links.lww.com/MD/B531>). For major details, see Methods section in the Supplements, <http://links.lww.com/MD/B531>.

Given the FGF/FGFR pathway positivity (Figs. 1 and 3), we designed a combined multitarget treatment. For 4 consecutive weeks the patient received: foscarnet (24 mg/mL IV) plus low molecular weight heparin (LMWH: 2.5 mg/0.5 mL subcutaneously) plus sunitinib (50 mg orally).

The experimental administration of multi-target therapy was approved by the Institutional Ethics Committee and Drug Committee.

Radiotherapy was applied to the scapula (20 Gy) and femur (30 Gy) while 20 Gy of high-energy electrons was directed at the neck.<sup>[14]</sup>

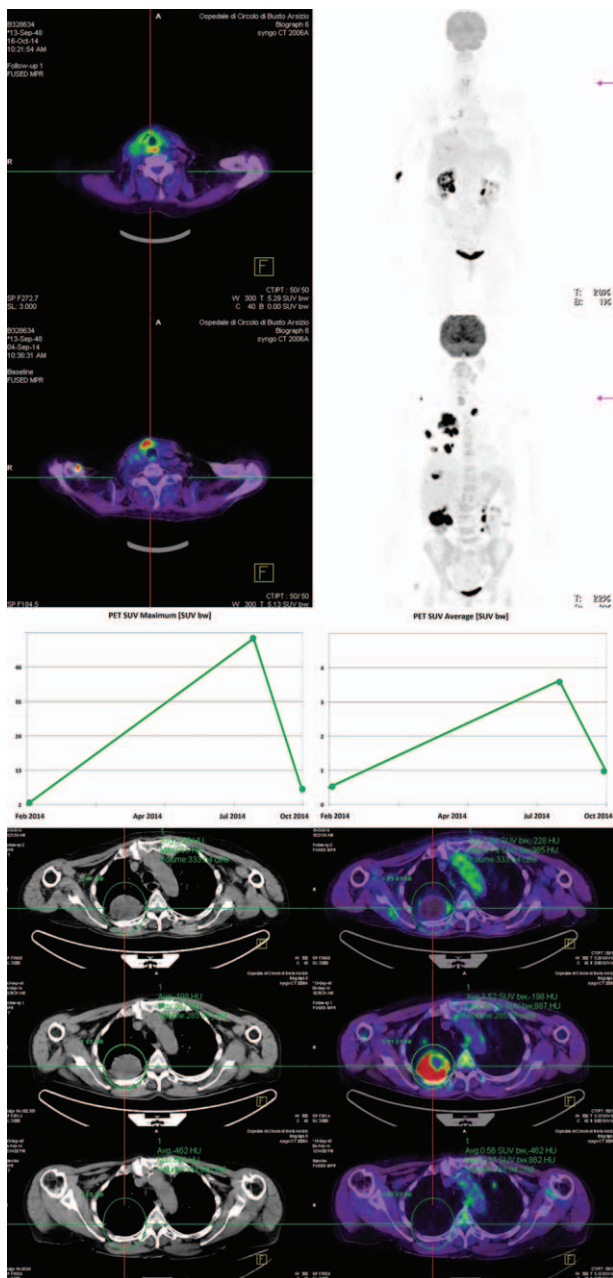


**Figure 2.** Whole body  $^{18}\text{F}$ -FDG PET/CT before and after multitarget therapy. A, It shows on the left, from bottom to top: complex PET/CT hybrid imaging of recurrence of pathological lesion in the right paramechanical cervical region and right scapula before (bottom) and after (top) systemic multi-target therapy (foscarnet + sunitinib + LMWH). On the right from bottom to top: whole-body PET/CT shows the extraordinary disappearance of pathological lesions 1 month after systemic multitarget therapy (foscarnet + sunitinib + LMWH). Black arrows indicate the main lesions in the right lung and kidney. B, Graphical and quantitative analysis of response to multitarget treatment according to PERCIST 1.0 criteria. On the right, a reduction in tumor standardized uptake value (SUV) over 200% from the starting value is detected 30 days after the start of multitarget therapy (foscarnet + sunitinib + LMWH). PERCIST 1.0 criteria defined a fractional change from the starting value of 20% in SUV of a region 1 cm or larger in diameter as statistically significant, and of 30% as clinically relevant. C, It shows, from bottom to center, the appearance of a pathological lesion in the right lung with central necrosis (visible on the right center of the image). At the top, 30 days after the start of multitarget therapy (foscarnet + sunitinib + LMWH): on the right, the pulmonary lesion appears completely functionally and metabolically silent on complex PET/CT imaging according to PERCIST 1.0 criteria, while on the left, anatomical imaging alone (according to RECIST criteria) is unable to measure the early response to the target therapy, showing a near identical mass to before. CT = computed tomography, LMWH = low molecular weight heparin, PERCIST = Positron Emission Tomography Response Criteria in Solid Tumors.

After the first cycle,  $^{18}\text{F}$ -FDG PET/CT documented a complete response to therapy in the neck, bones and lungs, and a significant improvement in the right kidney (Fig. 2A).

PERCIST 1.0 criteria determine that statistically significant changes in tumor standardized uptake value (SUV) occur with a 20% decline from the baseline SUV of a region 1 cm or larger in diameter; clinically relevant beneficial changes are often associated with a 30% decline.<sup>[15]</sup> The more effective the therapy, the greater the decline. Our multitarget treatment achieved a reduction of over 200% and disease remission in the neck (Fig. 2A and B); the main metastases were functionally silent on complex PET/CT imaging compared with anatomic imaging (Fig. 2C) at 30 days.

Unfortunately, a tracheal fistula appeared shortly thereafter and the patient's clinical condition deteriorated rapidly, despite protective tracheostomy. She died 13 months after diagnosis.

The flow chart of adopted therapies in timing action is shown in the Supplements (Fig. S2, <http://links.lww.com/MD/B531>).

### 3. Rationale for selected agents of multitarget therapy

#### 3.1. Foscarnet

Our case showed an up-regulation of FGF2, FGFR1, and FGFR4 proteins in primary ATC (Fig. 1), and significantly higher FGFR1 gene expression levels in the metastatic lymph node (Fig. 3). FGFR1 expression was recently correlated with increased phosphorylation status of pyruvate kinase M2 and lactate dehydrogenase A, contributing to faster proliferation in undifferentiated thyroid cancer.<sup>[16]</sup> We identify this agent in order to counteract tumor cell proliferation. Data about foscarnet activity in ATC cell line demonstrated a dose-dependent reduction of tumor cell proliferation without complete cell growth inhibition,<sup>[7]</sup> due to the simultaneous overexpression of other proliferation-inducing growth factors.

For this reason, we decided to act on different pathways.

#### 3.2. Low molecular weight heparin

LMWH was coadministered due to its role in limiting metastatic progression by interfering with tumor neo-angiogenesis.<sup>[17]</sup> Foscarnet interacts with FGF2 through the HBD, influencing FGF2-bioactivity and reducing ATC proliferation.<sup>[18]</sup> As FGF2 requires ATP binding in the HBD to intervene in cell growth, proliferation, and migration, and this is inhibited by heparin,<sup>[7]</sup> we hypothesized that LMWH potentiates the effects of foscarnet by competing with ATP binding. Interestingly, an HBD has also been identified on FGFR1.<sup>[19]</sup>

#### 3.3. Sunitinib

Sunitinib, a multitarget tyrosine kinase inhibitor, was administered as recommended by ATA guidelines.<sup>[20,21]</sup> Sunitinib has been reported as effective on neck tumor mass without significant impact on distant metastases, due to ATC heterogeneity, paradoxical responses, and selection of resistant clones.<sup>[22]</sup> The antiangiogenic effect of sunitinib concurrently with IMRT could normalize the tumor vascularization and enhance radiotherapy efficacy.<sup>[23]</sup>

### 4. Discussion

This report offers 2 new approaches: the first use of a combined therapy targeting FGF2 with foscarnet in a patient with ATC; a

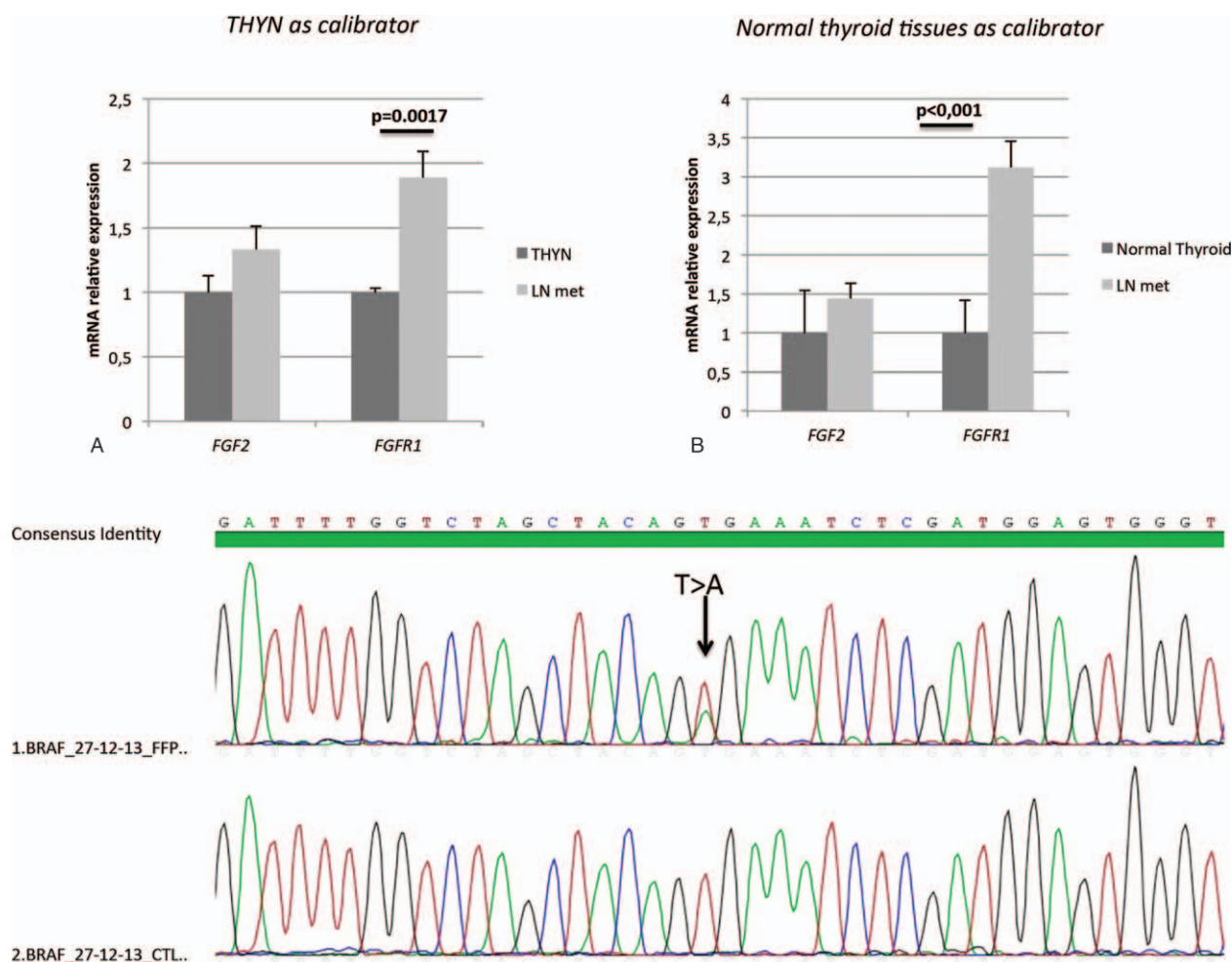


**Figure 3.** Genetic analyses. A (Top) shows sequence electropherogram for BRAFV600E mutation. The mutation found in the papillary thyroid cancer component is marked by an arrow, and the wild-type sequence of a control sample is shown below for comparison. B (Bottom) shows FGF and FGFR1 mRNA levels in a lymph node metastasis from anaplastic thyroid cancer. For each gene, the mRNA levels detected in the metastatic lymph-node tissue (LN met) of the patient (gray bars) are expressed as fold changes with respect to a calibrator, which has been assigned a value of 1. On the left, the calibrator is a commercial pool of normal thyroid tissues (THYN) and on the right it was the average of 5 normal thyroid tissues from our biobank (Normal Thyroid). Values are expressed as mean  $\pm$  SD.

prompt step-by-step clinical decisional process based on  $^{18}\text{F}$ -FDG PET/CT (PERCIST 1.0 criteria).

ATC is a rare, almost invariably fatal disease.<sup>[24]</sup> In the last years, detection of various mutations in ATC has allowed the employment of specific targeted therapies currently under clinical trial investigation.<sup>[25]</sup> However, resistance to treatment is far from solved.

Since our patient's ATC was negative for BRAF mutations<sup>[26]</sup> (Figs. 1–3) and ALK rearrangements (data not shown), and given the paucity of targetable pathways in ATC,<sup>[27]</sup> we explored the emerging role of FGF and the FGFR family as potential therapeutic targets in solid tumors.<sup>[28]</sup> The up-regulation of FGF2, FGFR1, and FGFR4 proteins in primary ATC, and the significantly higher FGFR1 gene expression levels in the metastatic lymph node gave reason of the inhibition of this specific target in our case. Given that FGFRs' modulation alone cannot arrest cell growth we decided to take action on several targets to control cell proliferation and growth.

So far, no data are available concerning long-term results of foscarnet administration in multitarget therapy in ATC patients.

We performed  $^{18}\text{F}$ -FDG PET/CT immediately after the treatment started, applying PERCIST 1.0 criteria as the biomarker

of cancer response to assess the treatments' efficacy.<sup>[15]</sup> After just 1 cycle of multitarget therapy the PERCIST criteria enabled an accurate measurement of the tumor's functional response (Fig. 2C) long before CT with RECIST criteria could have shown any anatomic response. The massive cell migration under foscarnet administration was quickly revealed, enabling the prompt shift to the new multitarget therapy (Fig. 2C). We supposed that foscarnet failed in our case for the drug-dependent yin-yang effect: a simultaneous suppression of cell proliferation and activation of cancer migration upon inhibition of a single signal pathway.

The remarkable response to therapy observed in our patient could be explained by the efficacy of the multitarget approach in blocking cell proliferation via the synergistic inhibition of ERK1/2 by foscarnet, LMWH and sunitinib, and cell migration via the sunitinib-dependent Akt modulation and LMWH activity.

As it is known ATC is a highly aggressive disease with short survival. In our case, we observed the failure of conventional therapy, and single-target therapy (foscarnet).

Despite the introduction of innovative multitargets therapy having produced extraordinary results in just 1 month of treatment, the onset of the death of our patient did not allow

extending the observation period of the efficacy of designed therapeutic scheme.

This is a limitation of our study.

We suggest in the clinical practice the introduction of gene expression analysis for FGF2 and FGFR1 and the relative immunostaining in each case of ATC.

In this context, in selected patients with positive FGF/FGFR pathway, after putting urgently in security the airways, foscavir could be coadministrated with LMWH. After short-term <sup>18</sup>F-FDG PET/CT assessment (1 month) with PERCIST 1.0 criteria, the physician may consider to customize the treatment with radiotherapy or sunitinib.

Larger studies aimed at analyzing the effectiveness of foscavir administration in selected patients with positive FGF/FGFR pathway in association or not to multitarget therapy with heparin and sunitinib are needed.

Unfortunately, the reduced survival of this disease represents per se a limit to a prolonged follow up.

Increased understanding of the biological mechanisms of acquired resistance and how to verify disease extension and response to therapy are necessary in order to produce stable and permanent remission in the most aggressive human cancers such as ATC.

## Acknowledgment

The authors thank Marie-Hélène Hayles for revision of the English text.

## References

- Smallridge RC, Copland JA. Anaplastic thyroid carcinoma: pathogenesis and emerging therapies. *Clin Oncol (R Coll Radiol)* 2010;22:486–97.
- Haymart MR, Banerjee M, Yin H, et al. Marginal treatment benefit in anaplastic thyroid cancer. *Cancer* 2013;119:3133–9.
- Sosa JA, Elisei R, Jarzab B, et al. Randomized safety and efficacy study of foscavir with paclitaxel/carboplatin against anaplastic thyroid carcinoma. *Thyroid* 2014;24:232–40.
- Sosa JA, Balkissoon J, Lu SP, et al. Thyroidectomy followed by foscavir (CA4P) combination regimen appears to suggest improvement in patient survival in anaplastic thyroid cancer. *Surgery* 2012;152:1078–87.
- Mooney CJ, Nagaiah G, Fu P, et al. A phase II trial of foscavir in advanced anaplastic thyroid carcinoma and correlation of baseline serum-soluble intracellular adhesion molecule-1 with outcome. *Thyroid* 2009;19:233–40.
- St Bernard R, Zheng L, Liu W, et al. Fibroblast Growth Factor receptors as molecular targets in thyroid carcinoma. *Endocrinology* 2005;146:1145–53.
- Rose K. Foscarnet reduces FGF2-induced proliferation of human umbilical vein endothelial cells and has antineoplastic activity against human anaplastic thyroid carcinoma cells. *Biomed Pharmacother* 2013;67:53–7.
- Schlumberger M, Tahara M, Wirth LJ, et al. Lenvatinib versus placebo in radioiodine-refractory thyroid cancer. *N Engl J Med* 2015;372:621–30.
- Yuan-Qu Y, Xiong-Pu M, Xiao-Kang J, et al. A comparison study on the clinical effects of foscarnet sodium injection and interferon on human immunodeficiency virus-infected patients complicated with herpes zoster. *Pak J Med Sci* 2015;31:309–13.
- Pugliese M, Fortunati N, Germano A, et al. Histone deacetylase inhibition affects sodium iodide symporter expression and induces 131I cytotoxicity in anaplastic thyroid cancer cells. *Thyroid* 2013;23:838–46.
- Takano T, Ito Y, Hirokawa M, et al. BRAF V600E mutation in anaplastic thyroid carcinomas and their accompanying differentiated carcinomas. *Br J Cancer* 2007;96:1549–53.
- Sponziello M, Durante C, Boichard A, et al. Epigenetic-related gene expression profile in medullary thyroid cancer revealed the overexpression of the histone methyltransferases EZH2 and SMYD3 in aggressive tumours. *Mol Cell Endocrinol* 2014;392:8–13.
- Puppin C, Durante C, Sponziello M, et al. Overexpression of genes involved in miRNA biogenesis in medullary thyroid carcinomas with RET mutation. *Endocrine* 2014;47:528–36.
- Foot RL, Molina JR, Kasperbauer JL, et al. Enhanced survival in locoregionally confined anaplastic thyroid carcinoma: a single-institution experience using aggressive multimodal therapy. *Thyroid* 2011;21:25–30.
- Wahl RL, Jacene H, Kasamon Y, et al. From RECIST to PERCIST: evolving considerations for PET response criteria in solid tumors. *J Nucl Med* 2009;50(suppl 1):122S–50S.
- Kachel P, Trojanowicz B, Sekulla C, et al. Phosphorylation of pyruvate kinase M2 and lactate dehydrogenase A by fibroblast growth factor receptor 1 in benign and malignant thyroid tissue. *BMC Cancer* 2015;15:140.
- Mousa SA, Petersen LJ. Anti-cancer properties of low-molecular-weight heparin: preclinical evidence. *Thromb Haemost* 2009;102:258–67.
- Rose K, Pallast S, Klumpp S, et al. ATP-binding on fibroblast growth factor 2 potentially overlaps the heparin-binding domain. *J Biochem* 2008;144:343–7.
- Kan M, Wang F, Xu J, et al. An essential heparin-binding domain in the fibroblast growth factor receptor kinase. *Science* 1993;259:1918–21.
- Smallridge RC, Ain KB, Asa SL, et al. American Thyroid Association guidelines for management of patients with anaplastic thyroid cancer. *Thyroid* 2012;22:1104–39.
- Di Desidero T, Fioravanti A, Orlandi P, et al. Antiproliferative and proapoptotic activity of sunitinib on endothelial and anaplastic thyroid cancer cells via inhibition of Akt and ERK1/2 phosphorylation and by down-regulation of cyclin-D1. *J Clin Endocrinol Metab* 2013;98:E1465–73.
- Gerling M, Rowan AJ, Horswell S, et al. Intratumor heterogeneity and branched evolution revealed by multiregion sequencing. *N Engl J Med* 2012;366:883–92.
- Schoenfeld JD1, Odejide OO, Wirth LJ, et al. Survival of a patient with anaplastic thyroid cancer following intensity-modulated radiotherapy and sunitinib: a case report. *Anticancer Res* 2012;32:1743–6.
- Baroli A, Pedrazzini L, Lomuscio G, et al. Anaplastic thyroid carcinoma: practical aspects of multimodal therapy and data emerging from 40-years experience at a single Italian institution. *Minerva Endocrinol* 2010;35:9–16.
- Ranganath R, Shah MA, Shah AR. Anaplastic thyroid cancer. *Curr Opin Endocrinol Diabetes Obes* 2015;22:387–91.
- Rosove MH, Peddi PF, Glaspy JA. BRAF V600E inhibition in anaplastic thyroid cancer. *N Engl J Med* 2013;368:684–5.
- Nikiforova MN, Wald AI, Roy S, et al. Targeted next-generation sequencing panel (ThyroSeq) for detection of mutations in thyroid cancer. *J Clin Endocrinol Metab* 2013;98:E1852–60.
- Parker BC, Engels M, Annala M, et al. Emergence of FGFR family gene fusions as therapeutic targets in a wide spectrum of solid tumours. *J Pathol* 2014;232:4–15.